7.4.3 Homogeneity in superconducting properties of the YBCO/Ag/YBCO joints

Now, for a better understanding of Ag diffusion phenomenon into YBCO matrix, we will determine the remanent magnetization profiles and critical current densities of different sample faces which will be called hereafter: top, center and bottom. It is important to notice that, since the resolution of the measurements depends on the distance between the Hall probe and the layer in which the critical current flows, not much information about the remanent magnetization distribution at the center and bottom sides is obtained by scanning the top face of the samples. Thus, in order to do this experiment we have cut the samples in three layers along the c-axis as it was schematically shown in figure 6.43. The ”top face” corresponds to the ab plane where the seed has been placed in order to obtain the YBCO monolith by TSMG process. The ”center” and ”bottom” faces correspond to ab planes situated at 0.3cm and 0.6cm below the ”top face”, respectively.

Two samples ΔT_{28} and C_3 obtained by the welding process have been chosen for the homogeneity study. The nomenclature used for the faces studied in this Section are $top_{\Delta 28}$ and top_{C_3}corresponding to the top side of the samples ΔT_{28} and C_3, respectively and $center_{\Delta 28}$, $center_{C_3}$ and $bottom_{\Delta 28}$, $bottom_{C_3}$ corresponding to the center and bottom sides of samples ΔT_{28} and C_3, respectively. Sample ΔT_{28} is a joint obtained after the optimization of the welding process by employing the following parameters: g_{Ag}=10μm thick, T_{max}=992°C, t_1=3h, T_2=973°C, t_2=1h, r=0.6°C/h, ΔT=28°C, T_{ox}=450°C and t_{ox}=168°C. On the contrary, sample C_3 is a joint obtained by using a non-optimized welding process, thus it is of a reduced critical current density. The later kind of joint is not of a technological interest but it will be interesting to determine the critical current density along its depth in order to observe the phenomenon of Ag diffusion and how does it affect the superconducting properties of the samples.

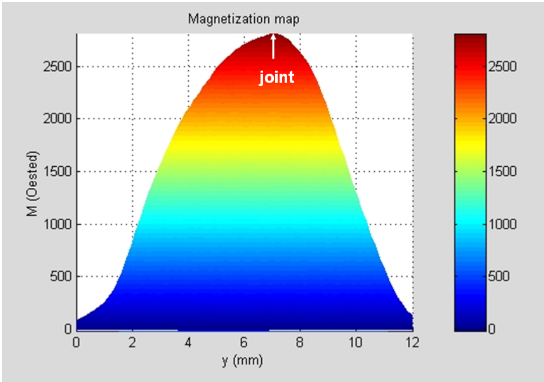

(a)

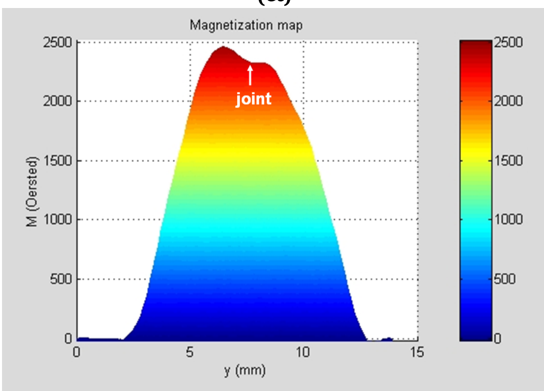

(a)

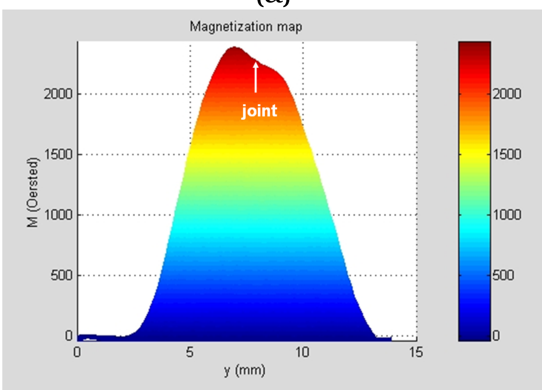

(b)

Figure 7.33: 2D remanent magnetization profiles obtained after a fc process for different faces along c-axis of the sample ΔT_{28}: a) top face, b) center face and c) bottom face. The center face is situated 0.3cm below the top face and the bottom face is situated 0.6cm below the top face. The dimension of c-axis of the top face is different from the other faces. The joint is indicated in the figure by arrows

.

"Top face" of the samples studied has a thickness of 0.6cm, whereas the center and bottom faces have a thickness of 0.3cm. As a consequence, the remanent magnetization at top faces cannot be compared with the remanent magnetization measured at center and bottom faces. We will use remanent magnetization measurements in order to have a general view of the quality of the final joint. For comparison purposes we will calculate the critical current density of the YBCO samples and of the final joints by using the software "Caragol".

The top face of sample ΔT_{28} was analyzed in order to optimize the parameter ΔT. It is shown that the remanent magnetization profile (figure 7.33a) exhibits only one peak, as expected for a single domain. As microstructural studies have shown (see figure 6.41), no additional phases have been formed at the interface after the welding process concluding that the profile indeed agrees with the results obtained when the microstructure was investigated. A small asymmetry is seen in this profile with respect to the joint, indicating a small difference between the critical current densities present in the sample in the left-hand side and right-hand side. Remanent magnetization profiles corresponding to center and bottom faces of sample ΔT_{28} are shown in figures 7.33(b-c), respectively, where the joint is indicated by arrows. A small reduction of remanent magnetization of the junction and of the YBCO grain from the right-side of the graph is observed in these profiles indicating that their critical current density are slightly reduced when compared with J_c of the left side YBCO grain. The inhomogeneity found in the remanent magnetization values is reflected in the critical current density values as can be seen in figure 7.34 where the blue and red symbols are associated with critical current density values corresponding to YBCO grains while the yellow symbols are associated to the critical current densities obtained for the junction.

Note that when, the top face is investigated, the critical current densities of the Grain 1 and Grain 2 are quite different. This difference make us conclude that the previous YBCO samples used for the joining process are in-

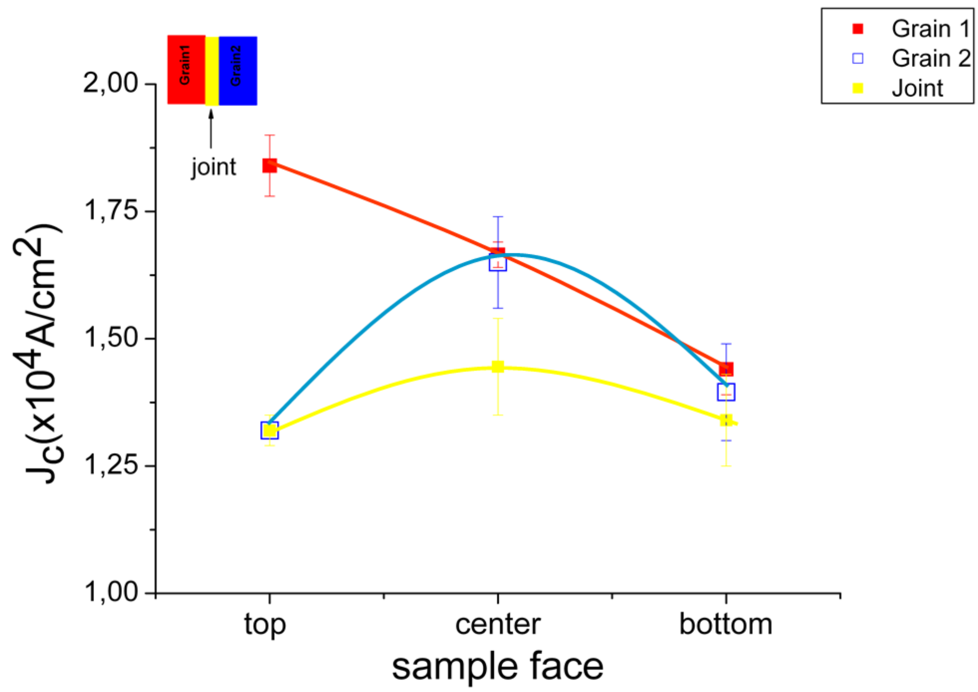

Figure 7.34: Critical current density values obtained along c-axis of the junction at different depths from the face, where the seed was located during the TS process. The sample analyzed is ΔT_{28}. Red and blue symbols indicate the critical current density dependence along the c-axis of the sample of the Grain 1 and Grain 2, respectively. Yellow symbols indicate this dependence for the joints. Error bars show the J_c values dispersion obtained by using the methodology detailed in Section 7.1.

homogeneous. The critical current density of the Grain 1 when the ”top face” was analyzed is J_c^{grain1}=1.84$\times 10^4 A/cm^2$ and of Grain 2 is J_c^{grain2}=1.35$\times 10^4 A/cm^2$. On the contrary, when the center and bottom faces are investigated, the critical current densities of Grain 1 and Grain 2 are J_c^{grain1}=1.67$\times 10^4 A/cm^2$, J_c^{grain2}=1.65$\times 10^4 A/cm^2$ and J_c^{grain1}=1.44$\times 10^4 A/cm^2$, J_c^{grain2}=1.4$\times 10^4 A/cm^2$, respectively and can be considered quite homogeneous.

Concerning the critical current density calculated at the junction we have noticed that the values determined all along its junction are similar. For the top face the critical current density is J_c^{gb}=$1.35 \times 10^4 A/cm^2$, for the center face is J_c^{gb}=$1.44 \times 10^4 A/cm^2$ and for the bottom face is J_c^{gb}=$1.34 \times 10^4 A/cm^2$. Thus, we can conclude that when the welding process is optimized, a quite homogeneous joint is obtained. For comparison purposes, we will determine the ratio J_c^{gb}/J_c^{grain} for each face studied. This ratio indicates the percentage of the reduction of the critical current density of joint (J_c^{gb}) after the welding process when compared with the lowest critical current density value obtain for the YBCO grains J_c^{grain} (see figure 7.34). The error bars in the figure quantify the dispersion on J_c^{gb}/J_c^{grain} values calculated by using the methodology described in Section 7.1 for each case and exist due mainly to the inhomogeneities found in the proper YBCO grains. For the top face note that J_c^{gb} exhibits similar value that the lowest critical current density exhibited by the YBCO grain, thus the ratio J_c^{gb}/J_c^{grain} is ~ 1 as it is indicated in the figure. On the contrary, note that for the center face, the ratio J_c^{gb}/J_c^{grain} is 0.87 which means that J_c^{gb} is reduced ∼12% from J_c^{grain}. Even the ratio is reduced, J_c^{gb} is kept constant. This reduction is given by the J_c^{grain2} increasing and not by the J_c^{gb} reduction. When the bottom face critical current density values are investigated, the ratio J_c^{gb}/J_c^{grain} is ∼0.96 which indicates that J_c^{gb} is reduced only 4% from J_c^{grain} values corresponding to the weakest grain. As it is shown in figure 7.34, the reduction of the J_c^{gb}/J_c^{grain} if it is compared with the ratio obtained for the top face and the enhancement of ratio value if it is compared with the ratio value obtained for the center face is mainly due the inhomogeneities in J_c values obtained for the YBCO grains.

Thus, we conclude that the J_c^{gb} is quite homogeneous along the c-axis and that the welding process used to determine this weld was the optimum one and Ag diffusion into YBCO matrix was quite homogeneous.

When the sample C_3 is investigated, differences in the remanent magnetization distribution between the top, center and bottom sides (see figures 7.36(a-c)) can be seen. All profiles exhibit two peaks indicating that the critical current which flows across the junction is disrupted by the inhomogeneities found at the interface when the microstructure has been investigated. In figure 6.47 (a-c) can be seen that some non-superconducting phases have been trapped at the

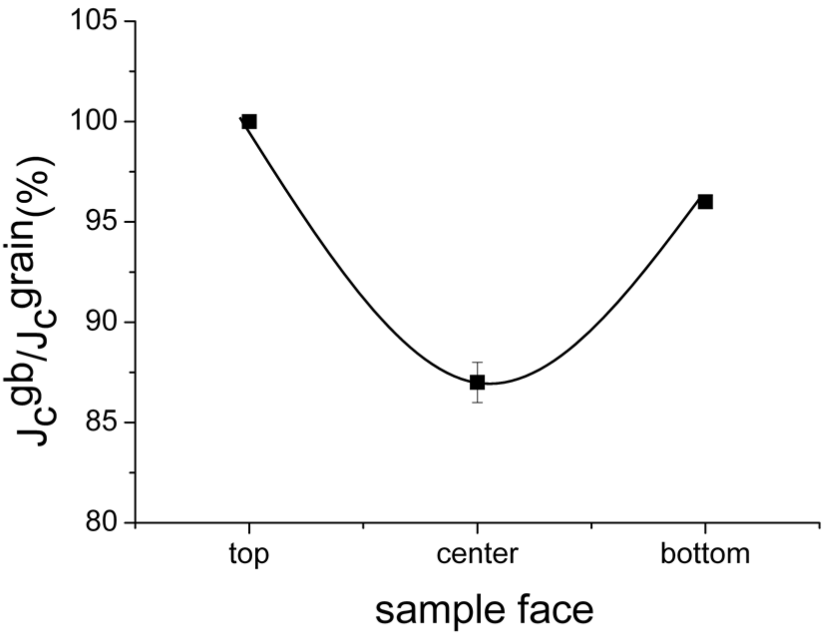

Figure 7.35: Dependence of ratio J_c^{gb}/J_c^{grain} with sample face analyzed (red and blue symbols for grains, whereas yellow symbols for the joint).

interface of the top face during the welding process. Because of the high cooling rate used to grow this sample, the Ag-rich liquid could not be completely eliminated from the interface and has solidified along with Y211 and $BaCuO_2 - CuO$ phases at the interface. On the contrary, the remanent magnetization profile corresponding to the center sample, $center_{C3}$, shows two less differentiated peaks indicating a better connectivity between grains than the other faces (center and bottom). As in the previous case when the sample ΔT_{28} was investigated, the top face of the sample is thicker than center and bottom faces, thus we cannot use the comparison as a method to conclude which face has higher performances. Because of this, we further continue our investigation by calculating the critical current density of the YBCO sample and final joint.

Critical current density values have been determined for sample C_3 by using

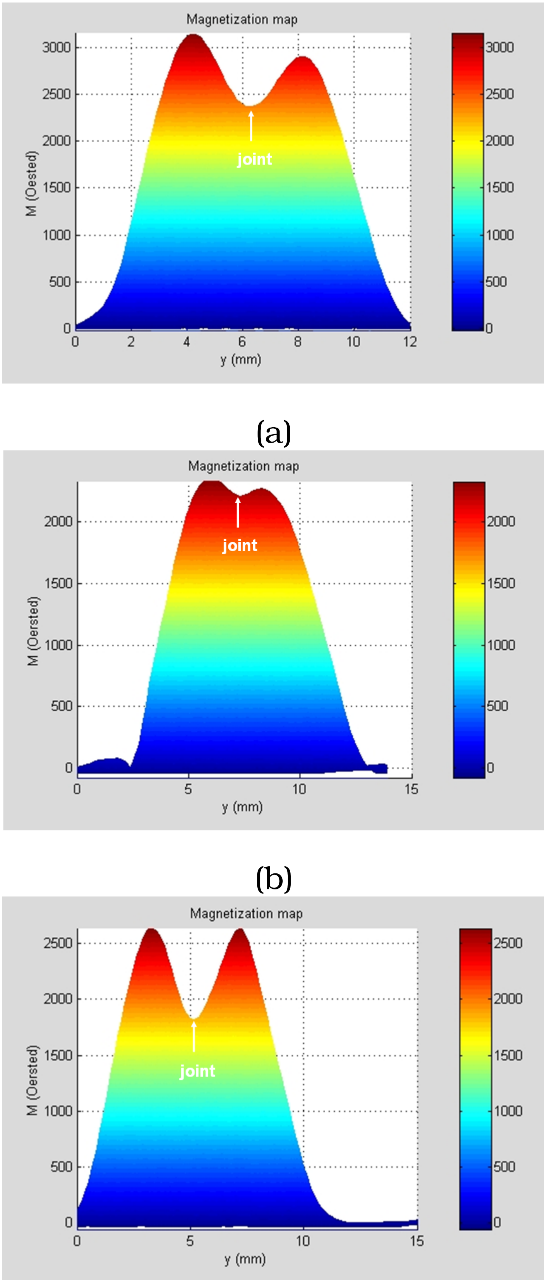

(a)

(b)

(c)

Figure 7.36: Remanent magnetization maps obtained after applying a field cooled process for different faces obtained along the c-axis of the sample C_3. a) top face, b) center face and c) bottom face. The center face is located at 0.3cm below the top face, whereas the bottom face is located at 0.6cm below the top face. The joints are indicated by arrows in the figure.

the methodology described in Section 7.1 and by using ”Caragol” software. Figure 7.37(a-c) shows the critical current density values determined for each side of sample C_3 (top, center and bottom) where red and blue symbols indicate the critical current density of the YBCO grains (Grain 1 and Grain 2) and the yellow symbols correspond to the J_c^{gb} values. Error bars in the figure quantify the inhomogeneity in J_c values found by employing this methodology. In the figure can be observed that the error bars indicating the dispersion of J_c values obtained for the YBCO grains are overlapping in all the cases. This can be interpreted as follows: this inhomogeneity in J_c values is mainly due to the inhomogeneity in the proper YBCO grains Thus, both YBCO grains could be considered of similar superconducting properties. The critical current density of the joint J_c^{gb} is spanning between $1.01 \times 10^4 A/cm^2$ and $1.21 \times 10^4 A/cm^2$. For the ”top face”, the critical current density of the junction is J_c^{gb}=$1.1 \times 10^4 A/cm^2$, whereas for the ”center face” is J_c^{gb}=$1.2 \times 10^4 A/cm^2$ and for the ”bottom face” J_c^{gb}=$0.8 \times 10^4 A/cm^2$. Higher reduction takes place at the bottom face.

The ratio J_c^{gb}/J_c^{grain} shows the percentage of the reduction of the critical current density of joint (J_c^{gb}) after the welding process when compare with the weakest YBCO grain. The dependence of this ratio with the analyzed face is depicted in figure 7.38. It can be observed that highest reduction of the critical current density of the joint took place for the bottom face of the J_c^{gb}/J_c^{grain} is ∼0.53 which means that J_c^{gb} is reduced ∼47% from the J_c^{grain} value corresponding to the lowest value of critical current density corresponding to YBCO grains. For the ”top face”, this ratio is ∼0.69, which means that J_c^{gb} value is reduced ∼31% from J_c^{grain2} value of sample C_3 where the ratio, whereas for the ”center face”, the figure shows that the J_c^{gb} was reduced ∼23% from the J_c^{grain2} value. As it was observed in figure 7.37, the critical current density values corresponding to the top and center faces of the junction are quite similar. On the contrary, the critical current density values corresponding to YBCO grain to the same faces showed a small inhomogeneity. Thus, we conclude that the difference in ratio values determined for the top and center faces of this sample is governed by the inhomogeneity in J_c values corresponding to proper YBCO grain and not to the differences in superconducting properties of both YBCO grains used for joining.

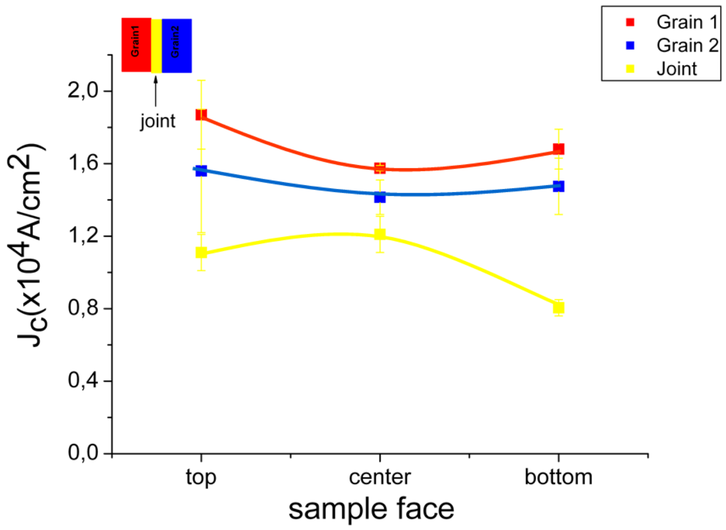

Figure 7.37: Critical current density values obtained for each YBCO grain (Grain 1 indicated by red symbols and Grain 2 indicated by blue symbols) and for the final joint (indicated by yellow symbols) along the c-axis of the joint. Top, center and bottom faces corresponding to the sample C_3 are investigated.

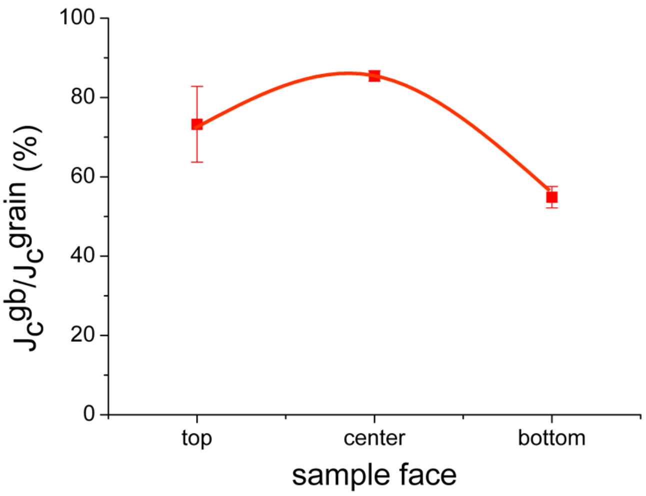

Figure 7.38: Ratio J_c^{gb}/J_c^{grain} along the c-axis of the sample analyzed. Top, center and bottom faces are investigated.

7.4.4 Conclusion of Chapter 7

The remanent magnetization distribution was investigated on samples joined by the welding process described in Chapter 5 by using a Hall probe imaging system. These measurements allow us to deduce the magnitude of the critical current densities by solving the inverse problem, i.e Biot-Savart law, as well as the homogeneity and spatial scale on which they flow.

We have proposed a methodology allowing the determination of the critical current density of the final joints from remanent magnetization profiles obtained by employing a Hall probe imaging system after a FC process. Following the Bean model which predicts that J_c is constant all over the sample, we have used only the y component of J_c (J_{cy}) to further determine the critical current density of the YBCO grains and of the junction at the same time. We have observed that the current distributions patterns obtained by using ”Caragol” software [30, 96] agree well with the current distribution profile predicted by the Bean model.

In this Chapter we have evaluated the limitations of the Hall probe imaging system, employed to determine the remanent magnetization profiles, and of the calculation of critical current densities by using the software ”Caragol”. In this way we have used a totally non-superconducting joint, obtained by simply gluing two YBCO parts. We have demonstrated that when the reduction in remanent magnetization of the joint with respect with YBCO grains, is higher than 60%-70%, the junction will be considered of a very low quality. Moreover, any sample exhibiting J_c values across the joint that have been reduced more than 60% after the welding process and an angle α higher than 33°, will be considered to have a low critical current density and we will not be able to quantify more precisely the J_c across the joint.

After the analysis performed on studied samples, we have observed that parameters such as: oxygenation time, cooling rate and window temperature are very important to optimize the quality of the superconducting joint. After the systematic analysis of the welding process, the samples obtained using the optimized parameters had pyramidal shaped remanent magnetization profiles, i.e they exhibit only one peak, indicating that the connectivity between the domains was good (example: sample ΔT_{28} and $C_{0.6}$). These samples exhibit only one current loop. When the welding process was not optimized some segregation of non-superconducting phases at the interface was observed with microstructural analysis. This segregation consists of a mixture of Ag-rich liquid which was not pushed complectly from the interface, Y211 and $BaCuO_2 - CuO$ phases which were trapped at the interface for different reasons which were explained in Chapter 6. Therefore, the critical current density flow was strongly limited at the junction and the remanent magnetization locally decreased (example: sample C_6). Consequently, some peaks and valleys appeared in the remanent magnetization profiles, which correspond to regions where the critical current flow was or was not limited, respectively. We have observed too that the difference in superconducting volume exhibited by the both YBCO grains used for joining is reflected in the remanent magnetization profiles obtained by using the Hall probe imaging system after a field-cooled process.

We have determined that: t_{ox}=168-240h, r≤ 1.8°C/h and ΔT=28°C are the optimum parameters needed for the obtention of a high quality superconducting joint and the critical current density of the junction determined by using the methodology described in Section 7.1 was J_c^{gb}=$1.35 \times 10^4 A/cm^2$, the same as the mother blocks. Moreover, it has been shown that the critical current density of the junction along the c-axis of the sample is quite homogeneous. On the contrary, J_c^{grain} of the YBCO material is quite inhomogeneous along c-axis. This inhomogeneity in J_c values is provided from the inhomogeneity in the microstructure of the starting samples. It has been shown that the inhomogeneity in the YBCO material is increasing while moving away from the top face of the sample, being the face where the seed has been placed during the TS method.

Chapter 8

Conclusions

The main goal of this PhD thesis has been to develop a technology which would be able to achieve superconducting pieces of large dimensions and complex geometries, with the purpose of integrating them into different superconducting devices by fabricating artificial superconducting joints.

The first step in achieving high temperature superconducting YBCO joints was to find a suitable welding material. We have investigated two Ag based materials as welding agents: Ag_2O powder and Ag thin foil. Microstructural analysis along with transport and in-field Hall mapping measurements have been performed to find the conditions to reach a high quality superconducting joints. Considering the quality limitations found with the use of Ag_2O powder as a welding agent, giving rise to the formation of a large amount of porosity at the interface, and the promising results achieved for Ag thin foils, we scheduled a systematic study of the YBCO joints parameters by using Ag thin foils as welding elements obtained by a cold rolling process.

A deep study of the influence of different parameters on the microstructure and on the superconducting properties, i.e remanent magnetization and critical current density of the final joints, generated using a YBCO/Ag/YBCO architecture has been performed in order to understand the role of the Ag diffusion and to optimize the welding process. It has been shown that these parameters influence in one way or another the microstructure and superconducting properties of the final joints. In order to optimize these parameters, we have preformed two kinds of experiments: quench experiments and slow cooling experiments. By quench experiments we have succeeded in controlling the Ag diffusion process into the YBCO matrix. Parameters such as: melting time (t_{melt}), Ag foil thickness (g_{Ag}) and weld configuration have been investigated and optimized. On the other hand, the influence of parameters such as: cooling rate (r), processing temperature (T_{max}) and window temperature (ΔT), on the microstructure of the final joints has been analyzed by means of slow cooling experiments.

It has been shown that the microstructure of the starting YBCO monoliths is very important since a strong Ag liquid migration from the interface occurs through the pre-existing macrocracks perpendicular to the interface. Hence, special care was taken to avoid the existence of such defects in the microstructure of the starting YBCO monoliths. We have used previously non-oxygenated samples which are mainly free, or have a reduced concentration of micro and macrocracks.

We have succeeded in controlling the Ag diffusion process into the YBCO matrix by employing a melting time of 3 hours, a Ag foil thickness of 10μm and a welding configuration (100)/(100). By using these conditions, the Ag diffusion is kept homogeneous and reduced in dimensions into the YBCO matrix.

By slow cooling experiments we have found that a T_{max}=992°C, a cooling rate of r=0.6°C/h and a window temperature of ΔT=28° are the optimum parameters for our samples, and thus they, should be used in order to obtain a clean welded interface free of impurities and pores and high critical current density joints. WDS analysis at the interface and far away from it have been performed. When the joint is obtained after applying an optimized welding process, no Ag precipitates have been detected neither at the interface nor into YBCO matrix. On the contrary, when the joint is obtained by using a non-optimized welding process, Ag-rich and Cu-rich precipitates have been detected at the interface.

Therefore, a 2D Ag diffusion model has been proposed after these analysis which establishes that Ag rich liquid is pushed away from the inner part of the sample towards its edges along the YBCO growth interface. The crystallization is first completed in the inner part where the Ag-rich liquid was completely expelled. It turns out, then, that we should use a cooling rate slow enough to expel all the Ag from the interface. Accumulation of non-superconducting phases, such as: Ag precipitates, Y211 and $BaCuO_2$ phases, at the edge of the junction occurs when the cooling rate (r) is too high and the time for recrystallization is too low.

The homogeneity in the microstructure of the final joints along the c-axis of the sample was analyzed. It was demonstrated that the microstructure at the interface was quite homogeneous along its depth.

The influence of welding process parameters on the superconducting properties of the final joints has been studied by determining the remanent magnetization profiles of each sample and calculating from them the critical current density of the joint and YBCO grains for comparison. Moreover, the ratio $J_c^{gb}/_c^{grain}$, indicating the reduction of critical current density of the joint with respect to the critical current density of the YBCO grains, has been calculated.

The remanent magnetization distribution was investigated on samples joined by the welding process by using a Hall probe imaging system. These measurements allowed us to deduce the magnitude of the critical current densities by solving the inverse problem by using the "Caragol" software, as well as the homogeneity and spatial scale on which they flow.

We have proposed a methodology in order to determine the critical current density of the final joints from the results of "Caragol". We have observed that the current distributions patterns obtained by using "Caragol" software agree well with current distribution profile predicted by Bean model.

We have determined the limitation of the Hall probe imaging system allowing the determination of the remanent magnetization profiles and of the calculation of the critical current densities by using the software "Caragol" by employing a glued sample. We have demonstrated that when the reduction in remanent magnetization of the joint with respect to the YBCO grains is higher than 60%-70%, the junction will be considered to be of a very low quality. Moreover, any sample exhibiting J_c values across the joint that have been reduced more than 60% after the welding process, will be considered to have a too low critical current density and we will not be able to quantify more precisely the J_c across the joint.

We have observed the influence of the following parameters: oxygenation time, cooling rate and window temperature on the remanent magnetization and critical current density of the final joints. We have determined that: t_{ox}=168-240h, r$\leq$ 1.8°C/h and ΔT=28°C are the optimum parameters needed for the obtention of high quality superconducting joint and the critical current density of the junction determined by using the methodology here proposed was J_c^{gb}=$1.35 \times 10^4 A/cm^2$, same as the mother blocks. These results agree with the results obtained when the microstructure of the final joints was investigated. Moreover, it has been shown that the critical current density of the junction along the c-axis of the sample is quite homogeneous. On the contrary, J_c^{grain} of the YBCO material is quite inhomogeneous along the c-axis. This inhomogeneity in J_c values is provided from the inhomogeneity in the microstructure of the starting material. It has been shown that the inhomogeneity in the YBCO starting material is increasing while moving down from the top face of the sample, being the top face where the seed was placed during the top seeding process.

In summary, by employing the new welding methodology developed in the present work, we have been able to obtain YBCO superconducting joints having a clean and crystallographic coincident microstructure and with critical current densities through the joint similar to those of the YBCO monoliths.

List of Figures

List of Tables

Bibliography

[1] M. Murakami, *Melt Processed High Temperature Superconductors*, vol. 21. 1992.

[2] S. Jin, T. H. Tiefel, R. C. Sherwood, M. E. Davis, R. B. van Dover, G. W. Kammlott, R. A. Fastnacht, and H. D. Keith *Appl. Phys. Lett.*, vol. 52, p. 2074, 1988.

[3] U. Wiesner, G. Krabbes, M. Ueltzen, C. Magerkurth, J. Plewa, and H. Altenburg *Physica C*, vol. 294, p. 17, 1998.

[4] Y. Nakamura, K. Tachibana, and H. Fujimoto *Physica C*, vol. 306, p. 259, 1998.

[5] E. Mendoza, T. Puig, E. Varesi, A. E. Carrillo, J. Plain, and X. Obradors *Physica C*, vol. 334, p. 7, 2000.

[6] M. P. Delamare, B. Bringmann, C. Jooss, H. Walter, A. Leenders, and H. C. Freyhardt *Supercond. Sci. and Technol.*, vol. 15, 2002.

[7] P. Schätzle, G. Krabbes, G. Stöver, G. Fuchs, and D. Schläfer *Supercond. Sci. and Technol.*, vol. 12, p. 69, 1999.

[8] K.Salama and V.Selvamanickam *Appl. Phys. Lett.*, vol. 60, p. 898, 1992.

[9] D. Shi *Appl. Phys. Lett.*, vol. 66, p. 2573, 1995.

[10] R. A. Doyle, A. D. Bradley, W. Lo, D. A. Cardwell, A. M. Campbell, P. Vanderbemden, and R. Cloots *Appl. Phys. Lett.*, vol. 73, p. 117, 1998.

[11] H. Zheng, M. Jiang, R. Nikolova, U. Help, A. P. Paulikas, Y. Huang, G. W. Crabtree, B. W. Veal, and H. Claus *Physica C*, vol. 322, p. 1, 1999.

[12] T. Puig, P. R. Jr., A. E. Carrillo, X. Obradors, H. Zheng, U. Welp, L. Chen, H. Claus, B. W. Veal, and G. W. Crabtree *Physica C*, vol. 363, p. 75, 2001.

[13] J. Yoshioka, K. Iida, T. Negichi, N. Sakai, K. Noto, and M. Murakami *Supercond. Sci. and Technol.*, vol. 15, p. 712, 2002.

[14] T. A. Prikhna, W. Gawalek, V. E. Moshchil, N. V. Sergienko, V. B. Sverdun, A. B. Surzhenko, M. Wendt, D. Litzkendorf, T. Habisreuther, and A. V. Vlasenko *Physica C*, vol. 386, p. 221, 2003.

[15] C. Harnois, G. Desgardin, and X. Chaud *Supercond. Sci. and Technol.*, vol. 14, p. 708, 2001.

[16] H. Walter, C. Jooss, F. Sandiumenge, B. Bringmann, M. P. Delamare, A. Leenders, and H. C. Freyhardt *Europhys. Lett.*, vol. 55, p. 100, 2001.

[17] M. P. Delamare, H. Walter, B. Bringmann, A. Leenders, and H. C. Freyhardt *Physica C*, vol. 329, p. 160, 2000.

[18] K. Iida, J. Yoshioka, N. Sakai, and M. Murakami *Physica C*, vol. 392-396, p. 437, 2003.

[19] L. Chen, H. Claus, A. P. Paulikas, H. Zheng, and B. W. Veal *Supercond. Sci. and Technol.*, vol. 15, p. 672, 2002.

[20] A. D. Bradley, W. Lo, M. Mironova, N. H. Babu, D. A. Cardwell, A. M. Campbell, and K. Salama *J. Mater. Res.*, vol. 16, p. 2298, 2001.

[21] A. A. Abrikosov *Soviet. Phys. JETP*, vol. 5, p. 1174, 1957.

[22] C. P. Bean *Phys. Rew. Lett*, vol. 8, 1962.

[23] J. D. Jorgensen, M. A. Beno, D. G. Hinks, L. Soderholm, K. J. Volin, R. L. Hitterman, J. D. Grace, I. K. Schuller, C. D. Segre, K. Zhang, and M. S. Kleefisch *Phys. Rew. B*, vol. 36, p. 3608, 1986.

[24] J. R. Clem *Supercond. Sci. Technol.*, vol. 11, p. 909, 1998.

[25] M. Tinhkam, *Introduction to Superconductivity.* Mc-Graw Hill, Inc., 2nd ed., 1996.

[26] D. E. Farrell, J. P. Rice, D. M. Ginsberg, and J. Z. Liu *Phys. Rev. Lett.*, vol. 64, p. 1573, 1990.

[27] K. E. Gray, R. T. Kampwirth, and D. E. Farrell: *Phys. Rev. B*, vol. 41, p. 819, 1990.

[28] J. C. Martinez, S. H. Brongersma, A. Koshelev, P. H. K. B. Ivlev, R. P. Griessen, D. G. D. Groot, Z. Tarnnavski, and A. A. Menovski *Phys. Rev.Lett.*, vol. 69, p. 2276, 1992.

[29] X. Granados, S. Sena, E. Bartolome, A. Palau, T. Puig, X. Obradors, M. Carrera, J. Amoros, and H. Claus *IEEE Trans. Appl. Supercond.*, vol. 13, p. 3667, 2003.

[30] M. Carrera, J. Amorós, X. Obradors, and J. Fontcuberta *Supercond. Sci. and Technol.*, vol. 16, p. 1187, 2003.

[31] M. Carrera, *Magnetometria Hall i deteminació de corrents critics en superconductors d´alta temperatura: $YBa_2Cu_3O_7$ texturat.* PhD thesis, Univ. de Barcelona, September 2003.

[32] B. Martinez, X. Obradors, A. Gou, V. Gomis, S. Pinol, J. Fontcuberta, and H. V. Tol *Phys. Rev. B*, vol. 53, p. 2797, 1996.

[33] K. Salama, V. Selvamanickam, L. Gao, and K. Sun *Appl. Phys. Lett.*, vol. 54, p. 2352, 1989.

[34] H. Hojaji, K. A. Michael, A. Barkatt, A. N. Thorpe, F. W. Matthew, I. G. Talmy, D. A. Haught, and S. Alterescu *J. Mater. Res.*, vol. 4, p. 28, 1989.

[35] F. Sandiumenge, S. Piñol, X. Obradors, E. Snoeck, and C. Roucou *Phys. Rev. B*, vol. 50, p. 7032, 1994.

[36] F. Sandiumenge, T. Puig, J. Rabier, J. Plain, and X. Obradors *Adv. Mat*, vol. 12, p. 375, 2000.

[37] P. Diko *Physica C*, vol. 363, p. 60, 2001.

[38] S. Sanfilippo, A. Sulpice, O. Laborde, D. Bourgault, T. Fournier, and R. Tournier *Phys. Rev. B*, vol. 58, p. 15189, 1998.

[39] C. J. Kim and G. Hong *Supercond. Sci. and Technol.*, vol. 12, p. R27, 1999.

[40] B. Martinez, X. Obradors, A. Gou, V. Gomis, S. Pinol, J. Fontcuberta, and H. V. Tol *Phys. Rev. B*, vol. 53, p. 2797, 1996.

[41] E. Mendoza, T. Puig, E. Varesi, A. E. Carrillo, J. Plain, and X. Obradors *Physica C*, vol. 334, p. 7, 2000.

[42] K. Sangwal, *Elementary crystal growth.* SAAN, 1994.

[43] J. C. Anderson, K. D. Leaver, R. D. Rawlings, and J. M. Alexander, *Materials Science.* Van Nostrand Reinhold Co. Ltd., 3rd ed., 1985.

[44] M. J. Cima, M. C. Flemings, A. M. Figueredo, M. Nakade, H. Ishii, H. D. Brody, and J. S. Haggerty *J. Appl. Phys.*, vol. 72, p. 179, 1992.

[45] T. Izumi, Y. Nakamura, and Y. Shiohara *J. Mater. Res.*, vol. 7, p. 1621, 1992.

[46] Y. Nakamura, K. Tachibana, S. Kato, T. Ban, S. I. Yoo, and H. Fujimoto *Physica C*, vol. 294, p. 302, 1998.

[47] T. Izumi and Y. Shiohara *J. Mater. Res.*, vol. 7, p. 16, 1992.

[48] M. Ullrich, D. Muller, K. Heinemann, L. Neil, and H. C. Freyhardt *Physica C*, vol. 198, p. 181, 1992.

[49] M. Morita, K. Miyamoto, K. Doi, M. Murakami, K. Sawano, and S. Matsuda *Physica C*, vol. 172, p. 383, 1990.

[50] S. Marinel, J. Wang, I. Monot, M. P. Delamare, J. Provost, and G. Desgardin *Supercond. Sci. and Technol.*, vol. 10, p. 147, 1997.

[51] D. R. Ulhmann, B. Chalmers, and K. A. Jackson *J. Appl. Phys.*, vol. 35, p. 2986, 1964.

[52] N. Vandewalle, M. Ausloos, and R. Cloots *J. Cryst. Growth*, vol. 197, p. 317, 1999.

[53] M. Ullrich, H. Walter, A. Leenders, and H. Freyhardt *Physica C*, vol. 311, p. 86, 1999.

[54] S. Kracunovska, P. Diko, D. Litzkendorf, T. Habisreuther, and W. Gawalek *Physica C*, vol. 397, p. 123, 2003.

[55] M. Murakami, M. Morita, K. Doi, K. Miyamoto, and H. Hamada *Jpn. J. Appl. Phys.*, vol. 28, p. 399, 1989.

[56] N. Vilalta, F. Sandiumenge, S. Pinol, and X. Obradors *J. Mater. Res.*, vol. 12, p. 38, 1997.

[57] S. Piñol, F. Sandiumenge, B. Martinez, V. Gomis, J. Fontcuberta, X. Obradors, E. Snoeck, and C. Roucau *Appl. Phys. Lett.*, vol. 65, p. 1448, 1994.

[58] R. Yu, F. Sandiumenge, B. Martinez, N. Vilalta, and X. Obradors *Appl. Phys. Lett.*, vol. 71, p. 413, 1997.

[59] P. Diko, G. Fuchs, and G. Krabbes *Physica C*, vol. 363, p. 60, 2001.

[60] J. Joo, J. Kim, and W. Nah *Supercond. Sci. and Technol.*, vol. 11, p. 645, 1998.

[61] G. Fuchs, G. Krabbes, P. Schatzle, P. Stoye, T. Staiger, and K. Muller *Physica C*, vol. 268, p. 115, 1996.

[62] G. Fuchs, P. Schatzle, G. Krabbes, S. Gruss, P. Verges, K.-H. Muller, J. Fink, and L. Schultz *Appl. Phys. Lett.*, vol. 76, p. 2107, 2000.

[63] A. Goyal, P. Funkenbusc, D. Kroeger, and S. Burns *Physica C 203*, vol. 182, p. 203, 1991.

[64] J. Maeda, T. Izumi, and Y. Shiohara *Supercond. Science and Technol.*, vol. 12, p. 232, 1999.

[65] T. Habisreuther, D. Litzkendorf, O. Surzhenko, M. Zeisberger, R. Muller, J. Riches, S. Schauroth, J. Dellith, and W. Gawalek *IEEE Trans. Appl. Supercond.*, vol. 11, p. 1163, 2001.

[66] M. Ullrich, H. Walter, A. Leenders, and H. C. Freyhardt *Physica C*, vol. 311, p. 86, 1999.

[67] J. G. Noudem, E. S. Reddy, E. A. Goodilin, M. Tarka, M. Noe, and G. J. Schmitz *Physica C*, vol. 372-376, p. 1187, 2002.

[68] S. Iliescu, X. Granados, E. Bartolomé, S. Sena, A. E. Carrilllo, T. Puig, X. Obradors, and J. E. Evetts *Supercond. Sci. and Technol.*, vol. 17, p. 182, 2004.

[69] S. Iliescu, S. Sena, X. Granados, E. Bartolomé, T. Puig, X. Obradors, M. Carrera, J. Amorós, S.Krakunovska, and T. Habisreuther *IEEE Trans. Appl. Supercond.*, vol. 13, p. 3136, 2003.

[70] G. Crabtree, W.K.Kwok, U. Help, D. Lopez, and J. Frendrich *Physics and Materials Science of vortex states, flux pinning and dynamics*, vol. 356, 1999.

[71] T. Puig, F. Galante, B. Martinez, X. Obradors, E. Gonzalez, and J. L. Vicent *Phys. Rev. B*, vol. 60, p. 13099, 1999.

[72] M. Tomita and M. Murakami *Nature*, vol. 421, p. 517, 2003.

[73] B. Bozzo, X. Granados, T. Puig, and X. Obradors *to be published*.

[74] P. Diko and G. Krabbes *Supercond. Sci. and Technol.*, vol. 16, p. 90, 2003.

[75] D. Shi, P. Odier, A. Sulpice, D. Isfort, X. Chaud, R. Tournier, P. He, and R. Singh *Physica C*, vol. 384, p. 149, 2003.

[76] K. Salama and S. Sathyamurthy *Supercond. Sci. Technol.*, vol. 11, p. 954, 1998.

[77] X. Obradors, R. Yu, F. Sandiumenge, B. Martinez, N. Vilalta, V. Gomis, T. Puig, and S. Pinol *Supercond. Sci. Technol.*, vol. 10, p. 884, 1997.

[78] T. Habisreuther, D. Litzkendorf, O. Surzhenko, M. Zeisberger, R. Muller, J. Riches, S. Schauroth, J. Dellith, and W. Gawalek *IEEE Trans. Appl. Supercond*, vol. 11, p. 3501, 2001.

[79] R. Tournier, E. Beaugnon, O. Belmont, X. Chaud, D. Bourgault, D. Isfort, L. Porcar, and P. Tixador *Supercond. Sci. Technol.*, vol. 13, p. 886, 2000.

[80] A. K. Gangopady¡hyay and T. O. Mason *Physica C*, vol. 178, p. 64, 1991.

[81] J. Joo, J. P. Singh, R. B. Poeppel, A. K. Gangopadhyay, and T. O. Mason *J. Appl. Phys.*, vol. 71, p. 2351, 1992.

[82] T. Izumi, Y. Nakamura, and Y. Shiohara *J. Mater. Res.*, vol. 8, p. 1240, 1993.

[83] N. Vilalta, F. Sandiumenge, S. Pinol, and X. Obradors *J. Mater. Res.*, vol. 12, p. 38, 1997.

[84] D. R. Uhlmann, B. Charlmers, and K. A. Jackson *J. Appl. Phys.*, vol. 35, p. 2986, 1964.

[85] A. Endo, H. S. Chauhan, T. Egi, and Y. Shiohara *J. Mater. Res*, vol. 11, p. 795, 1996.

[86] M. P. Delamare, H. Walter, B. Bringmann, A. Leenders, and H. C. Freyhardt *Physica C*, vol. 323, p. 107, 1999.

[87] C. J. Kim, K. B. Kim, I. H. Kuk, and G. W. Hong *J. Mater. Res.*, vol. 13, p. 269, 1998.

[88] A. E. Carrillo, T. Puig, J. Plain, J. Figueras, and X. Obradors *Physica C*, vol. 336, p. 213, 2000.

[89] P. Diko, W. G. andT. Habisreuther, T. Klupsch, and P. Görnert, vol. 52. Phys. Rev. B, 1995.

[90] G. K. Perkins, Y. Bugoslavski, X. Qi, J. L. MacManus-Driscoll, and A. D. Caplin *IEEE Trans. on Appl. Supercond.*, vol. 11, p. 3186, 2001.

[91] R. Gonzalez, *Trapped field characterization in neutron irradiated (RE)BCO melt-textued superconductors*. PhD thesis, Atominstitut der Osterreichischen Universitaten, 2002.

[92] C. Jooss, J. Albrecht, H. Kuhn, S. Leonhardt, and H. Kronmuller *Rep. Prog. Phys.*, vol. 65, p. 651, 2002.

[93] A. A. Polyanskii, A. Gurevich, A. E. Pashitski, N. F. Heinig, R. D. Redwing, J. E. Nordman, and D. C. Larbalestier *Phys. Rev. B*, vol. 53, p. 8687, 1996.

[94] K. Kowano, J. S. Abell, A. D. Bradley, W. Lo, and A. Campbell *Supercond. Sci. Technol.*, vol. 13, p. 999, 2000.

[95] C. Jooss, J. Albrecht, H. Kuhn, and H. Krommuller, *Magneto-optical studies of current distributions in High-T_c superconductors*. Review article.

[96] "On line at: www.jaumetor.upc.es."

[97] P. Vanderbemden, A. D. Bradley, R. A. Doyle, W. Lo, D. M. Astill, D. A. Cardwell, and A. M. Campbell *Physica C*, vol. 302, p. 257, 1998.

[98] W. Assmus and W. Schmidbauer *Supercond. Sci. and Technol.*, vol. 6, p. 555, 1993.

[99] F. Sandiumendge and J. Rabier, *Studies of high temperature superconductors*, ch. 28. a. v. narlikar, nova science, n. y ed., 1999.

[100] P. Diko *Supercond. Sci. Technol.*, vol. 13, p. 1202, 2000.